LAWRENCE
LIVERMORE
NATIONAL
LABORATORY

LLNL-JRNL-657541

Pattern Recognition with Composite Correlation Filters Designed with Multi-object Combinatorial Optimization

A. Awwal

July 22, 2014

Optics Communications

Disclaimer

This document was prepared as an account of work sponsored by an agency of the United States government. Neither the United States government nor Lawrence Livermore National Security, LLC, nor any of their employees makes any warranty, expressed or implied, or assumes any legal liability or responsibility for the accuracy, completeness, or usefulness of any information, apparatus, product, or process disclosed, or represents that its use would not infringe privately owned rights. Reference herein to any specific commercial product, process, or service by trade name, trademark, manufacturer, or otherwise does not necessarily constitute or imply its endorsement, recommendation, or favoring by the United States government or Lawrence Livermore National Security, LLC. The views and opinions of authors expressed herein do not necessarily state or reflect those of the United States government or Lawrence Livermore National Security, LLC, and shall not be used for advertising or product endorsement purposes.

Pattern recognition with composite correlation filters designed with multi-objective combinatorial optimization

Victor H. Diaz-Ramirez[1], Andres Cuevas[1] , Vitaly Kober[2], Leonardo Trujillo[3], and Abdul Awwal[4]

[1] *Instituto Politécnico Nacional - CITEDI, Ave. del Parque 1310, Mesa de Otay, Tijuana B.C. 22510, Mexico*
[2] *Department of Computer Science, CICESE, Carretera Ensenada-Tijuana No. 3918, Ensenada, B.C. 22860, Mexico*
[3] *Instituto Tecnológico de Tijuana, Ave. Tecnológico, Tijuana, B.C, 22414 México*
[4] *National Ignition Facility, Lawrence Livermore National Laboratory, Livermore, California 94551, USA*

Abstract

Composite correlation filters are used for solving a wide variety of pattern recognition problems. These filters are given by a combination of several training templates chosen by a designer in an ad-hoc manner. In this work, we present a general approach for the design of composite filters based on multi-objective combinatorial optimization. Given a vast search space of feasible training templates, an iterative algorithm is used to synthesize a filter with an optimized performance in terms of several criteria. Moreover, by using a suggested binary search procedure a filter bank with a minimum number of filters is constructed, for a given trade-off of performance metrics. Computer simulation results obtained with the proposed approach in recognizing geometrically distorted versions of a target in cluttered and noisy scenes, are discussed and compared in terms of recognition performance and complexity with existing state-of-the-art filters.

Keywords: Object recognition, composite correlation filters, multi-objective evolutionary algorithm, combinatorial optimization.

1. Introduction

Nowadays, object recognition receives much research interest due to its high impact in real-life activities, such as, robotics, biometrics, and target tracking [1, 2]. Object recognition consists in solving two essential tasks: detection of a target within an observed scene, and determination of the exact position of the detected object. Different approaches can be utilized to address these tasks; that is, feature-based methods [3–6] and template matching algorithms [7, 8]. In feature-based methods the observed scene is processed to extract relevant features of potential targets within the scene. Next, the extracted features are processed and analyzed to make decisions. Feature-based methods yield good results in many applications. However, they depend on several subjective decisions which often require optimization [9, 10]. On the other hand, correlation filtering is a template matching processing. In this approach, the coordinates of the maximum of the filter output are taken as estimates of the target coordinates in the observed scene. Correlation filters possess a good mathematical foundation and they can be implemented by exploiting massive parallelism

either in hybrid opto-digital correlators [11, 12] or in high-performance hardware such as graphics processing units (GPUs) [13] or field programmable gate arrays (FPGAs) [14] at high rate. Additionally, these filters are capable to reliably recognize a target in highly cluttered and noisy environments [8, 15, 16]. Moreover, they are able to estimate very accurately the position of the target within the scene [17]. Correlation filters are usually designed by a optimization of various criteria [18, 19]. The filters can be broadly classified in two main categories: analytical and composite filters. Analytical filters optimize a performance criterion using mathematical models of signals and noise [20, 21]. Composite filters are constructed by combination of several training templates, each of them representing an expected target view in the observed scene [21, 22]. In practice, composite filters are effective for real-life degradations of targets such as rotations and scaling. Composite filters are synthesized by means of a supervised training process. Thus, the performance of the filters highly depends on a proper selection of image templates used for training [20, 23]. Commonly, the training templates are chosen by a designer in an ad-hoc manner. Note that such a subjective procedure is not optimal. Additionally, Kumar and Pochavsky [24] showed that the signal to noise ratio (SNR) of a composite filter gradually reduces when the number of training templates increases. In order to synthesize composite filters with improved performance in terms of several competitive metrics, a search and optimization strategy is required to automatically choose the set of training templates.

To achieve this goal, we propose an iterative algorithm based on multi-objective combinatorial optimization. Given a vast search space of feasible training templates, the algorithm finds a subset of these templates that allows the synthesis of a composite filter with an optimized performance in terms of several objective metrics. Additionally, by employing a suggested binary-search procedure a bank of composite filters can be constructed using a minimum number of filters for a prespecified trade-off performance among various metrics. The proposed design algorithm combines two evolutionary computation techniques. Firstly, population management is performed by the Strength Pareto Evolutionary Algorithm 2 (SPEA2) [25], which is a state-of-the-art multi-objective evolutionary algorithm (MOEA). Secondly, individuals of the population are represented as variable length strings, while genetic operators applied to individuals are managed by the Speciation Adaptation Genetic Algorithm (SAGA) [26].

The proposed design algorithm allows the synthesis of composite filters as a trade-off between several competitive criteria. With the help of the obtained Pareto fronts we show that there is a trade-off between the discrimination capability of the designed filter, the tolerance of the filter to geometrical distortions of the target, and the signal to noise ratio of the filter. Also, we show through computer simulations that the composite filters designed by the proposed algorithm yield a superior recognition performance than common correlation filters. The designed filters possess also a lower computational complexity than that of common composite filters.

The paper is organized as follows. Section 2 presents a brief review of composite correlation filters for object recognition. We recall synthetic discriminant functions (SDF) [27], optimal trade-off SDF (OTSDF)

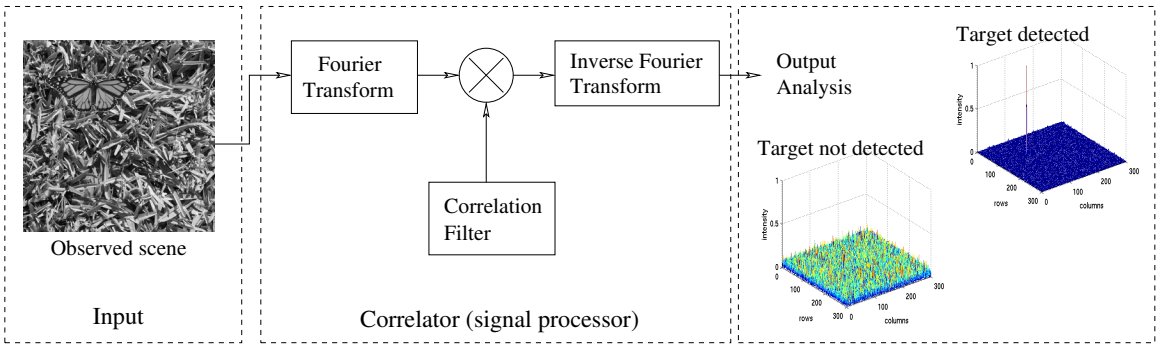

Figure 1: Block diagram of a basic system for pattern recognition with correlation filters.

filters [28], and the minimum output sum of squared error (MOSSE) filter [29]. Section 3 explains the proposed multi-objective approach for filter design. Section 4 presents the results obtained with the proposed composite filters for object recognition and classification problems. The obtained results are analyzed and discussed in terms of objective measures and computational complexity. These results are also compared with those obtained with existing correlation filters. Finally, section 5 summarizes our conclusions.

2. Composite correlation filters for robust object recognition

Object recognition by correlation filtering consists in calculation of the cross-correlation function between an observed image and the impulse response of a linear filter [20]. Next, the coordinates of the maximum of the cross-correlation are obtained. If the maximum is greater than a prespecified threshold, the obtained coordinates are taken as estimates of the target location in the observed scene; otherwise, the object is rejected. This process is depicted in Fig. 1. A desirable feature of correlation filters is that they can be robust to disjoint and overlapping noise as well as to geometrical degradations of a target [30, 31]. We review three different successful approaches for the design of composite correlation filters. The considered approaches are as follows: synthetic discriminant functions (SDF) [22], optimal trade-off SDF (OTSDF) [28], and minimum output sum of squared error (MOSSE) [29] filters.

2.1. Synthetic discriminant functions (SDF)

Let $T = \{t_i(x,y); i = 1, \ldots, N\}$ be a set of N different training templates, where each of them represents a distorted version of the target $t(x,y)$. A common composite filter is designed to recognize the target and all its views in T with a single linear correlation. A SDF filter is given by a linear combination of training images $t_i(x,y)$, as follows:

$$h(x,y) = \sum_{i=1}^{N} a_i t_i(x,y), \tag{1}$$

where $\{a_i; i = 1, \ldots, N\}$ are weighting coefficients that must be chosen to satisfy the inner-product conditions [22],

$$c_i = \langle t_i(x,y), h(x,y) \rangle . \tag{2}$$

The quantities $\{c_i; i = 1, \ldots, N\}$ are prespecified constraints imposed to the correlation output of the filter, at the origin for each training image. Let $\mathbf{T}$ be a matrix with N columns and d rows (d is the number of pixels in each training image) where its ith column is given by $\mathbf{t}_i$, which is a $d \times 1$ vector constructed by placing elements of $t_i(x, y)$ in lexicographical order. Let $\mathbf{a}$ and $\mathbf{c}$ represent column vectors of $\{a_i\}$ and $\{c_i\}$, respectively. Using matrix-vector notation, the impulse response of the filter $h(x, y)$ and constraints $\{c_i\}$ can be rewritten as

$$\mathbf{h}_{\mathrm{SDF}} = \mathbf{T}\mathbf{a}, \tag{3}$$

and

$$\mathbf{c} = \mathbf{T}^{+}\mathbf{h}_{\mathrm{SDF}}, \tag{4}$$

where superscript "+" denotes conjugate transpose. By substitution of Eq. (3) into Eq. (4) the solution of the system of equations is $\mathbf{a} = (\mathbf{T}^{+}\mathbf{T})^{-1}\mathbf{c}$, and if the matrix $(\mathbf{T}^{+}\mathbf{T})$ is nonsingular, the filter solution is

$$\mathbf{h}_{\mathrm{SDF}} = \mathbf{T}\left(\mathbf{T}^{+}\mathbf{T}\right)^{-1}\mathbf{c}. \tag{5}$$

Now, assume that there are several distorted versions of the target $\{t_i(x, y); i = 1, \ldots, N_T\}$ and various objects to be rejected $\{f_i(x, y); i = 1, \ldots, N_F\}$. In other words, we have a two-class pattern recognition problem. The goal is to design a SDF filter capable to recognize images from the true-class set (target class) given by $T = \{t_1(x, y), \ldots, t_{N_T}(x, y)\}$, and reject patterns from the false-class (unwanted class), given by $F = \{f_1(x, y), \ldots, f_{N_F}(x, y)\}$. A two-class composite filter can be constructed by combining all given training images in a set $U = T \cup F$. In order to solve the two-class problem we set the filter's constraints in Eq. (2) as $\{c_i = 1; i = 1, 2, \ldots, N_T\}$ for the true-class objects, and $\{c_i = 0; i = N_T + 1, N_T + 2, \ldots N_T + N_F\}$ for the false-class objects. In this manner the vector $\mathbf{c}$ is given by

$$\mathbf{c} = \left[\underbrace{1, 1, \ldots, 1}_{N_T \text{ ones}}, \underbrace{0, 0, \ldots, 0}_{N_F \text{ zeros}}\right]^{T}. \tag{6}$$

A SDF filter with equal output correlation peaks can be used either for intraclass distortion-tolerant pattern recognition (one class recognition) or for interclass pattern recognition (two class recognition). For two-class problems, we expect that the central correlation peak for each filter will be close to unity for the true-class objects and close to zero for objects of the false-class. Note that this approach can be easily extended to multi-class problems [7].

2.2. Optimal trade-off SDF (OTSDF) filter

Note that a main drawback of the SDF filter is the appearance of sidelobes in the output correlation plane that reduce the filter's performance. This problem can be solved by minimizing the average correlation energy (ACE) of the output plane except at the coordinates of the correlation peak. Let $\hat{\mathbf{t}}_i$ and $\hat{\mathbf{f}}_i$, be both $d \times 1$ vectors obtained by reordering elements (lexicographically) of the Fourier transforms of the training

images $t_i(x,y)$ and $f_i(x,y)$, respectively. Let $\mathbf{X}_i$ and $\mathbf{M}$ be both $d \times d$ diagonal matrices containing elements of the vector $\hat{\mathbf{t}}_i$, and the average vector $\mathbf{m} = \frac{1}{N}\sum_{i=1}^{N}\hat{\mathbf{t}}_i$, respectively. The ACE is given by

$$\mathrm{ACE} = \frac{1}{dN}\sum_{i=1}^{N}\left|\mathbf{v}_i\right|^2, \tag{7}$$

where $\mathbf{v}_i = \mathbf{X}_i^*\mathbf{h}$ is the output correlation plane generated by the filter $\mathbf{h}$ in response to the ith training image. A desirable feature of a composite filter is its ability to yield tolerance to intraclass distortions. The average similarity measure (ASM) is a measure of the robustness of a filter to intraclass distortions. The ASM is given by the average squared error between the full correlation responses produced by the filter for true-class training images, and the output correlation plane generated by the average training image, given by $\bar{\mathbf{v}} = \mathbf{M}^*\mathbf{h}$. The ASM is given by

$$\mathrm{ASM} = \frac{1}{dN}\sum_{i=1}^{N}\left|\mathbf{v}_i - \bar{\mathbf{v}}\right|^2. \tag{8}$$

The OTSDF filter is designed to provide an optimal performance in terms of a trade-off among various performance criteria [28, 32]. Using matrix-vector notation, the ACE and ASM measures can be rewritten as

$$\mathrm{ACE} = \mathbf{h}^+\mathbf{D}\mathbf{h}, \tag{9}$$

and

$$\mathrm{ASM} = \mathbf{h}^+\mathbf{S}\mathbf{h}, \tag{10}$$

where

$$\mathbf{D} = \frac{1}{dN}\sum_{i=1}^{N}\mathbf{X}_i\mathbf{X}_i^*, \tag{11}$$

and

$$\mathbf{S} = \frac{1}{dN}\sum_{i=1}^{N}\left(\mathbf{X}_i - \mathbf{M}\right)\left(\mathbf{X}_i - \mathbf{M}\right)^*. \tag{12}$$

The OTSDF filter avoids hard constraints imposed to the correlation peak (unconstrained filter) like the ones used in the SDF design. Instead, the OTSDF filter maximizes the average correlation height (ACH) of correlation peaks for the true-class training images. The ACH is given by

$$\mathrm{ACH} = \mathbf{m}^+\mathbf{h}. \tag{13}$$

The OTSDF filter is obtained by minimizing the following function [28]:

$$\begin{aligned} J(\mathbf{h}) &= \omega_1\mathrm{ACE} + \omega_2\mathrm{ASM} - |\mathrm{ACH}| \\ &= \omega_1\mathbf{h}^+\mathbf{D}\mathbf{h} + \omega_2\mathbf{h}^+\mathbf{S}\mathbf{h} - \left|\mathbf{h}^+\mathbf{m}\right|, \end{aligned} \tag{14}$$

where ACE and ASM are functions to be minimized, ACH is a function to be maximized, and $\left(\omega_1^2 + \omega_2^2 = 1\right)$ are trade-off coefficients. Note, that ACE and ASM measures are competitive objectives. The OTSDF filter

is obtained by [28]

$$\mathbf{h}_{\mathrm{OTSDF}} = \left(\omega_2 \mathbf{D} + \omega_2 \mathbf{S}\right)^{-1} \mathbf{m}. \tag{15}$$

2.3. Minimum sum of squared error (MOSSE) filter

The MOSSE filter [29] is designed to produce prespecified correlation planes $g_i(x, y)$ for a given set of available true-class training images $t_i(x, y)$. The MOSSE filter is obtained by minimizing the following functional:

$$\mathbf{h}_{\mathrm{MOSSE}} = \underset{\mathbf{h}}{arg\,min} \left\{ \sum_{i=1}^{N_T} \left| \mathbf{X}_i^* \mathbf{h} - \mathbf{g}_i \right|^2 \right\}, \tag{16}$$

where $\mathbf{g}_i$ is a $d \times 1$ vector containing elements of the Fourier transform of $g_i(x, y)$. The MOSSE filter is given by [29]:

$$\mathbf{h}_{\mathrm{MOSSE}} = \left(\sum_{i=1}^{N_T} \mathbf{X}_i^* \mathbf{X}_i \right)^{-1} \left(\sum_{i=1}^{N_T} \mathbf{X}_i^* \mathbf{g}_i \right). \tag{17}$$

3. Filter design by multi-objective combinatorial optimization

In this section, we describe the proposed approach for the synthesis of composite correlation filters for robust target recognition. The filters are designed to yield tolerance to geometrical distortions of the target, as well as to scene perturbations given by additive and disjoint noise. Conventional design schemes, such as the OTSDF, characterize scene perturbations in terms of ASM and ACE measures. Note that both of these measures are based on calculation of spatial averages. Thus, they only work well for stationary noise processes. In a real-life application, the stationary assumption of noise processes may not be valid. To overcome this problem, we use stricter criteria than ASM and ACE to quantify the effects of common scene disturbances. We are also interested in optimizing the number of training images used for the filter synthesis. So, the metrics considered for the design of composite filters are explained below.

Discrimination Capability (DC): The DC characterizes the ability of a filter to distinguish between a target and false-class objects [7]. For composite filter design, the DC can be defined as

$$DC = MIN \left\{ \left(1 - \frac{|c_F|^2}{\left|c_T^i\right|^2} \right); i = 1 \ldots, N_T \right\}, \tag{18}$$

where c_F is the maximum cross-correlation value in the area occupied by false-class objects (maximum sidelobe) and c_T^i is the maximum correlation value in the response to the ith target view (correlation peak). DC values close to unity indicate that the filter has a good capacity to distinguish the target from any false-class object. Negative values of the DC indicate that the filter is unable to recognize the target.

Maximum Absolute Error (MAE): The MAE is used to characterize the tolerance of a composite filter to intraclass distortions of the target. The MAE is defined as the maximum error between the correlation peaks $\left\{c_T^i\right\}$ obtained by the filter in response to different target views, and the constraints imposed by the

designer to the correlation peaks. If the peak constraints are all equal to unity, the MAE can be expressed by

$$MAE = MAX\left\{\left|c_T^i - 1\right|; i = 1\ldots, N_T\right\}. \tag{19}$$

Signal to Noise Ratio (SNR) [18, 24]: The SNR is a measure of the robustness of a correlation filter to input noise. The SNR is defined as the ratio between the intensity of the expected value of the correlation peaks $\left\{c_T^i\right\}$ to the peaks variance; i.e.,

$$SNR = \frac{\left|E\left\{c_T^i\right\}\right|^2}{var\left\{c_T^i\right\}}. \tag{20}$$

For composite filters, it has been shown [24] that the SNR is closely related to the number of training images of the filter. Thus, the SNR can be maximized by minimizing the number of training images of the filter.

In a real-life application, all expected target views can be seen as a true-class set of patterns to be recognized by the filter. Similarly, the background and any undesired objects can be considered as a false-class set of patterns to be rejected. In this two-class scenario, the best filter to be designed should exhibit a trade-off performance among the DC, MAE, and SNR metrics. Formally, such filter is not unique, and the solution is composed by a set of optimal solutions called the Pareto set [33]. A particular filter, can be completely and uniquely determined by the set of training templates taken from the true and false classes. Therefore, the design of optimal filters can be posed as a combinatorial optimization problem, using a Pareto-based multi-objective formulation. The following subsections describe the proposed methodology and search strategies to automatically design correlation filters.

3.1. Problem statement: Multi-objective combinatorial optimization problem

Let T be a finite set consisting of different views of the target (true-class templates), and let F be the set of image templates that constitute the false-class[1]. For instance, let us assume that the true-class templates are given by geometrically distorted versions of the target. Moreover, the false-class templates in F can be given by known false objects to be rejected and by unknown patterns having similar structures to those of the target. If the properties of the expected background in a real application are known, the false class templates can be given by small fragments taken from a synthetic image with similar statistical characteristics to those of the expected background. Suppose that the distorted versions of the target are given by in-plane rotations within the interval of [-180, 180] degrees and that the scene image has $M \times M$ pixels. Then, the set T contains a total of $N_T = 361$ templates taken with the angle step of one. Since a fragment of the background used to construct a false-class template can be extracted at any coordinate of the synthetic background image used for training [7], the set F contains at least $N_F = M \times M \times 361$ image templates. Under this scenario, the total number of feasible templates is $N_U = N_T + N_F$. Furthermore, to

[1] In general, the set F is infinite, because the number of possible undesired patterns is infinite. However, in practice F is a finite set of false patterns determined a priori.

synthesize a SDF filter as specified in Eq. (5), a particular combination of false and true class templates from set $U = T \cup F$ is required. Stated in these terms, the design of an optimal filter can be posed as a combinatorial optimization problem. The solution space $\mathcal{S}$ is given by all possible combinations formed by elements of set U. Hence, the size of the solution space is given by

$$|\mathcal{S}| = \sum_{r=1}^{N_U} \frac{N_U!}{r!\,(N_U - r)!}\ , \tag{21}$$

where r is the number of templates used in a particular combination. Note that even for a relatively small U, the solution space is extremely large, that makes exhaustive search unfeasible.

Let $\mathbf{P} = \{\mathbf{p}_1, \mathbf{p}_2, \ldots, \mathbf{p}_r\}$ define a particular subset (combination) of elements from U; i.e., $\mathbf{P}$ is a composite filter or solution to the problem, with $\mathbf{P} \in \mathcal{S}$ and $\mathbf{p}_i \in U$. Using three performance metrics defined in the preceding section, the performance of the filter specified by $\mathbf{P}$ is given by the objective vector $J(\mathbf{P})$ defined as

$$J(\mathbf{P}) = [DCm(\mathbf{P}), MAE(\mathbf{P}), SNRm(\mathbf{P})], \tag{22}$$

where $DCm = 1 - DC$ and $SNRm = 1 - \frac{1}{1+SNR}$, to pose all criteria as objectives to be minimized. In this manner, the problem of designing an optimal composite filter $\mathbf{P}^O$ can be stated as

$$\mathbf{P}^O = \underset{\mathbf{P}\in\mathcal{S}}{arg\,min}\,\{J(\mathbf{P})\}. \tag{23}$$

Note that $\mathbf{P}^O$ represents an optimal combination of training templates given in terms of the objective vector $J(\mathbf{P})$, where all criteria are competitively minimized.

The problem defined in Eq. (23) seems straightforward; however, it also exhibits two challenging properties. First, space $\mathcal{S}$ contains feasible solutions of different sizes r, ranging from 1 to $|U|$. Second, the criteria defined in J represent competitive objectives, since they cannot be minimized simultaneously. Therefore, a proper solution strategy should explicitly contemplate a multi-objective search with a variable length encoding. In this sense, the proposal of this work is to use a genetic algorithm with a variable length representation, guided by a Pareto-based multi-objective selection strategy.

3.2. Variable length Evolutionary Algorithm

Evolutionary algorithms (EAs) are population based search and optimization strategies [34]. In general, an EA is an iterative algorithm where an initial set (population) of candidate solutions (individuals) are randomly generated and evaluated based on a given set of performance measures or objectives (fitness). Then, some of the solutions are chosen (selection) and used to generate new candidate solutions with search operators (crossover and mutation). Finally, the best solutions are kept (survival) for the following iteration (generation) of this general cycle. In this process, both selection and survival are done probabilistically with preference to those individuals that exhibit the best performance. Moreover, the search operators are stochastic functions, that randomly modify and/or combine previously found solutions to generate new ones.

EAs have proven to be powerful search strategies in problems with large, multimodal and highly irregular or discontinuous search spaces, or when gradient information is not trivially computed [34].

To successfully apply an EA to the filter design problem, the following aspects must be defined. First, a search space $\mathcal{G}$ must be specified, in which $\forall \mathbf{P} \in \mathcal{S}\ \exists \mathbf{g} \in \mathcal{G} \mid y(\mathbf{g}) = \mathbf{P}$, where y is a mapping function. In other words, $\mathcal{G}$ represents an encoding scheme for solutions in $\mathcal{S}$. For the present problem, $\mathcal{G}$ is defined as the set of all possible combinations of U, such that $y : \mathcal{G} \rightarrow \mathcal{S}$ is a many to one mapping, for every possible combination of size r. In particular, the proposed system employs the representation specified by the Speciation Adaptation Genetic Algorithm (SAGA) technique developed by Harvey [26]. In SAGA, candidate solutions are represented by variable length strings $\mathbf{g} = \{g_1, g_2, \ldots, g_r\}$, where each $\mathbf{g}$ represents a combination of elements from a finite alphabet Σ, such that there is one-to-one correspondence between Σ and U.

The second component of an EA is to define a set of search operators $O_{n,m}$ of the form $O_{n,m} : \mathcal{G}_1 \times \cdots \times \mathcal{G}_n \rightarrow \mathcal{G}_1 \times \cdots \times \mathcal{G}_m$, where n represents the arity of the operator and m is the number of new solutions it generates. For instance, the most common operators are $O_{1,1}(\mathbf{g})$ which is referred to as a mutation, and $O_{2,2}(\mathbf{g}_1, \mathbf{g}_2)$ referred to as a crossover. These search operators take n feasible solutions, referred to as parents, and produce new candidate solutions which are referred to as offspring. In general, a search operator $O_{n,m}$ is defined in such a way to promotes two distinct outcomes. Firstly, the offspring should exhibit similar characteristics to those of the parents; this is known as inheritance. Secondly, the offspring should also exhibit (slight) variations with respect to the parents. This allows the algorithm to explore new regions within the search space. In particular, SAGA employs the following search operators. For crossover, a crossing point i within the first parent string $\mathbf{g}_1$ is chosen randomly. This defines two regions within $\mathbf{g}_1$, let us call them the left region $\mathbf{g}_1^{i,L} = \{g_1, \ldots, g_i\}$ and the right region $\mathbf{g}_1^{i,R} = \{g_{i+1}, \ldots, g_r\}$. Then, SAGA tests each possible crossing point j from the second parent string $\mathbf{g}_2$, based on the longest common sub-sequence (LCSS) metric, that measures the length of the longest non-interrupted matching sequence of symbols between two strings of arbitrary length. In other words, the crossing point in the second parent string j' is chosen as follows:

$$j' = arg \max_{j} \left\{ LCSS(\mathbf{g}_1^{i,L}, \mathbf{g}_2^{j,L}) + LCSS(\mathbf{g}_1^{i,R}, \mathbf{g}_2^{j,R}) \right\}. \tag{24}$$

SAGA assures that a meaningful crossover occurs between parent strings, where $O_{2,2}(\mathbf{g}_1, \mathbf{g}_2)$ produces two offspring, $\mathbf{g}_1' = \mathbf{g}_1^{i,L}, \mathbf{g}_2^{j',R}$ and $\mathbf{g}_2' = \mathbf{g}_2^{j',L}, \mathbf{g}_1^{i,R}$, each composed by the splicing of the left and right parts of different parents. Since the crossing points in each parent string may be in a different position the resultant strings can have different lengths.

The final component in an EA can be referred to as population management; i.e. the manner in which candidate solutions are selected to be used as parents, and to determine which individuals survive and are used in the following iteration. In general, such choices should be based on the corresponding objective

vector J of each solution; however, care must be taken given the conflicting nature of the considered metrics.

3.3. Multi-objective optimization

Multi-objective optimization is substantially more complex than single criterion optimization, considered as a separate field of research. The difference between single and multi-objective optimization resides with how the concept of optimality is defined. In single objective optimization the concept of optimality is trivially defined in a monodimensional space. In multi-objective optimization the optimality is based on dominance relations among solutions being evaluated in a multidimensional space [33].

In multi-objective optimization it is necessary to consider two different and complimentary spaces explicitly: one for decision variables and another for the objective functions. In the case of real valued functions, these two spaces are related by the mapping $\vec{f} : \mathcal{R}^n \rightarrow \mathcal{R}^k$. The set of constraints on the objective vector $\vec{f}(\mathbf{x}) = (f_1(x), ..., f_k(x))$ defines a feasible region $\Omega \subset \mathcal{R}^n$ in the decision space along with its corresponding image $\Lambda \subset \mathcal{R}^n$ on the objective function space. Now, the following concepts define the optimality for a multi-objective problem.

Pareto dominance: *Given k objectives and $N = \{1, ..., k\}$, an objective vector $\vec{f}^u$ is said to dominate another objective vector $\vec{f}^v$* (written as $\vec{f}^u \preceq \vec{f}^v$) $\Leftrightarrow \ \forall\, i \in N,\ f_i^u \leq f_i^v \ \wedge\ \exists\, j \in N \mid \ f_j^u < f_j^v$.

Pareto optimality: *A solution vector $\mathbf{x}^* \in \Omega$ is optimal if $\forall\, \mathbf{x} \in \Omega$ it is true that $\forall\, i \in N,\ f_i(\mathbf{x}) = f_i(\mathbf{x}^*) \vee \exists\, i \in N |\ f_i(\mathbf{x}) > f_i(\mathbf{x}^*)$.*

Pareto-Optimal Set: *For a multiobjective problem $\vec{f}(\mathbf{x})$, the set of Pareto optimal solutions* is $\mathcal{P}^* := \left\{\mathbf{x} \in \Omega \ \ \nexists\, \mathbf{x}' \in \Omega \ s.t.\ \vec{f}(\mathbf{x}) \preceq \vec{f}(\mathbf{x}')\right\}$.

Pareto Front: *For a multiobjective problem $\vec{f}(\mathbf{x})$ with a Pareto optimal set $\mathcal{P}^*$, the Pareto Front is defined as $\mathcal{PF}^* := \{\mathbf{u} = (f_1(\mathbf{x}), ..., f_k(\mathbf{x})) | \mathbf{x} \in \mathcal{P}^*\}$.*

For the filter design problem, decision space is given by $\mathcal{S}$ and objective space is defined by the objective vector J. Then, the goal of the search process would be to find all Pareto-optimal filters $\mathbf{P}^* \in \mathcal{P}^*$ instead of a single global optimum $\mathbf{P}^O$ as defined in Eq. (23). Moreover, the optimality is based on Pareto-dominance relations given by the objective vector specified by J.

3.3.1. MOEA: Multi-objective Evolutionary Algorithm

As stated above, when several competitive objectives are optimized concurrently, a single optimal solution cannot exist. On the contrary, there is a set of multiple feasible solutions, and all are optimal in the Pareto sense. Therefore, a multi-objective EA (MOEA) should fulfill the following: (1) it must converge towards the true Pareto Front; and (2) it must representatively sample the true Pareto Front.

Over the last years, MOEAs have proven to be powerful and robust strategies for multi-objective problems, particularly since MOEAs rely on a population based search which is well suited to search for multiple solutions concurrently; i.e., the Pareto-optimal set. While many algorithms were proposed (see [35] for a recent survey), most MOEAs follow the same basic design principles. Firstly, fitness assignment must

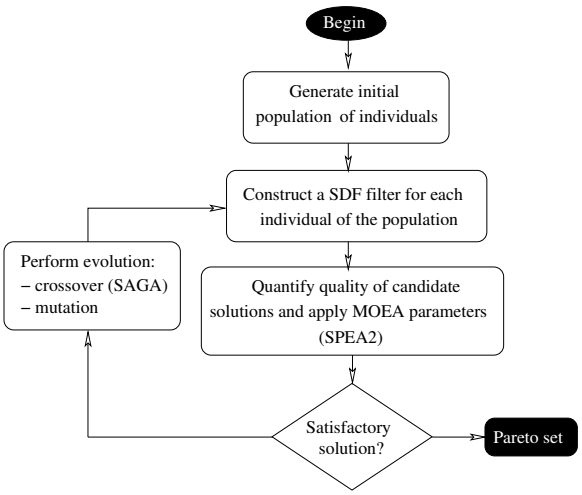

Figure 2: Basic block diagram of proposed multi-objective algorithm.

considers Pareto dominance relations to rank individuals. Secondly, because a close to uniform sampling of the true Pareto Front is desired, diversity of solutions within the evolutionary algorithm are encouraged, where similarity within objective space is penalized. Thirdly, to bias the search towards the Pareto Front, elitism is encouraged (where the best solutions of each generation are maintained) by employing some form of population archive, storing all non-dominated solutions found during the search.

In this work, the Improved Strength Pareto Evolutionary Algorithm (SPEA2) is used to guide the search [36]. SPEA2 is a third generation MOEA, an improved version of the second generation SPEA [37]. SPEA2 selects solutions based on dominance and non-dominance relations, between an individual and individuals in both the current population and the population archive. Diversity preservation is done using a k-th nearest neighbor clustering algorithm that penalizes solutions that lie in densely populated regions of objective space. SPEA2 uses a fixed-size archiving approach, and a truncation scheme promotes diversity by removing individuals that have the minimum distance to their neighbors. Finally, it preserves boundary solutions by using a carefully designed selection operator. The main drawback of SPEA2 is its diversity preservation method, with a time complexity of $O(N^3)$ where N is the population size. Nevertheless, the overhead is negligible for problems where fitness assignment bears a high computational cost, as is the case for the problem posed in this work.

3.4. Multi-objective filter design algorithm: SPEA2+SAGA

The proposed SPEA2+SAGA algorithm is shown in Fig. 2, and proceeds as follows. The first step is to construct an initial population of individuals, where each is a combination of image templates taken from set U. This population is randomly generated and each individual is coded using constant length strings. The quality of each individual is quantified in terms of J, following the procedure shown in Fig. 3. In this figure, the image templates specified by the individual are used to construct $\mathbf{P}$. Afterwards, $\mathbf{P}$ is used to

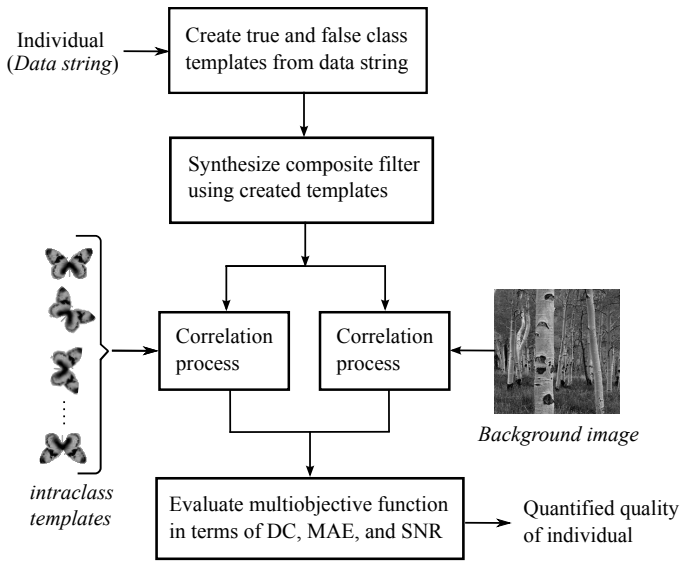

Figure 3: Block diagram of the process for evaluation of quality of a potential solution.

synthesize a two-class SDF filter. The correlation process is carried out between the filter and several target views (true-class samples), as well as with the synthetic image of the background (false-class). The DC, MAE, and SNR metrics are computed from the resultant correlation planes; i.e., vector $J(\mathbf{P})$. SPEA2 is then used to rank the individuals, and select those that will be used by the SAGA operators to generate new candidate solutions. If a subset of the chosen individuals satisfy a prespecified goal, then the algorithm finishes; otherwise the algorithm performs another iteration. The resultant filters can be implemented in the processing architecture shown in Fig. 1.

3.5. Automated design of a bank of composite filters for robust target recognition

The proposed design algorithm of Fig. 2 can generate robust filters, but to obtain a good pattern recognition performance on real-life applications a bank of composite filters is often required. For the design of a pattern recognition system two important factors should be considered. First, the pattern recognition system should yield a good recognition performance in terms of reliability, efficiency, and robustness. Second, the system should possess a low computational complexity. In object recognition by correlation filters, the computational complexity can be characterized by the number of linear correlations needed for recognition of a target in the scene. We count correlations because represent the most time-consuming operation among others used in the recognition process. Using the proposed MOEA algorithm shown in Fig. 2, we can synthesize composite filters with a good tolerance to geometrical distortions of a target for a prescribed range of expected intraclass distortions. In order to construct a filter bank, a different search strategy is needed to determine the minimum number of correlation filters. To design such a filter bank, we propose an iterative algorithm based on binary search [38], whose flow-diagram is depicted in Fig. 4. Suppose that the

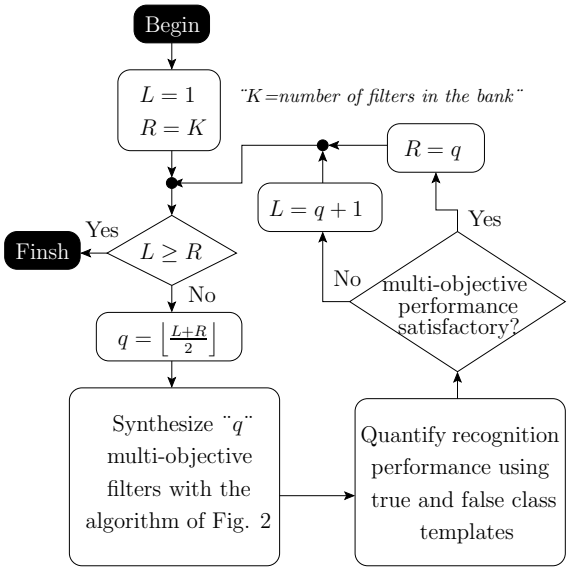

Figure 4: Proposed algorithm to construct a bank of multi-objective composite filters.

designed filter bank should be capable to recognize a target within the interval of $[-180, 180]$ degrees. Also, assume that a single composite filter synthesized with the proposed MOEA algorithm is able to recognize the target with a tolerance of ± 5 degrees and with a DC value of about 0.9. Note that to construct a filter bank with the DC performance of about 0.9, 36 composite filters are required. If the DC value is reduced to 0.8, then we need less than 36 filters. In this case, the computational complexity of the recognition system will be lower. To determine the minimum number of filters in a filter bank and at the same time satisfy a prespecified performance in terms of the DC or a trade-off among several criteria, the binary search algorithm shown in Fig. 4 can be used.

4. Results

In this section results obtained with composite correlation filters designed by the proposed multi-objective optimization algorithm are discussed in terms of efficiency of target detection, accuracy of target localization, and pattern classification. These results are compared with those obtained with successful state-of-the-art composite filters, the OTSDF [28, 32] and MOSSE [29] filters. The composite filters are tested within the context of target recognition and pattern classification problems. Object recognition, consists of detection of a target in an input scene and in estimating the location of the target within the scene. Pattern classification is given by detecting a target from a scene and in the assignment of the detected target to a corresponding category. The detection performance of the tested filters is characterized by the DC (see Eq. (18)). The accuracy of location estimation of the target is measured in terms of location errors (LEs) [17], as follows:

$$LE = \left[(\tau_x - \hat{\tau}_x)^2 + (\tau_y - \hat{\tau}_y)^2 \right]^{1/2}, \tag{25}$$

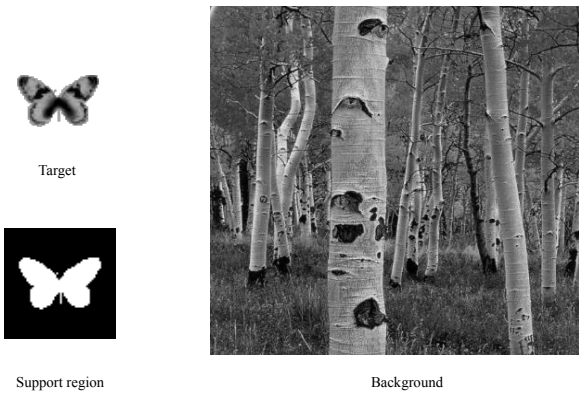

Figure 5: Test patterns used in target recognition experiments.

where (τ_x, τ_y) and $(\hat{\tau}_x, \hat{\tau}_y)$ are exact and estimated coordinates, respectively, of the target within the scene. The test patterns used for target recognition are shown in Fig. 5. The input scene is represented according to the nonoverlapping signal model, given by

$$f(x,y) = t(x-\tau_x, y-\tau_y; \rho, \phi) + b(x,y)\bar{w}(x-\tau_x, y-\tau_y; \rho, \phi) + n(x,y), \tag{26}$$

where $t(x-\tau_x, y-\tau_y; \rho, \phi)$ denotes a target (small butterfly) embedded into the background $b(x,y)$ at unknown coordinates (τ_x, τ_y), and having a scale factor ρ and a orientation angle ϕ. The function $\bar{w}(x,y)$ is the inverse region of support of the target (see Fig. 5) given by unity outside the target area and zero elsewhere, and $n(x,y)$ is a zero-mean additive noise with the variance of σ_n^2. All images are monochrome, with 400×400 pixels, a signal range of $[0,1]$, and 256 quantization levels. The target has the size of 72×36 pixels, a mean value of $\mu_t = 0.26$, and a standard deviation of $\sigma_t = 0.13$. The background image has the mean value of $\mu_t = 0.23$ and the standard deviation of $\sigma_b = 0.17$.

We designed five filter banks of SDF filters using the multi-objective algorithm depicted in Fig. 2. We call these filters multi-objective SDF (MOSDF) filters. The designed filter banks are composed by 30, 18, 12, 9, and 5 MOSDF filters, respectively. It is evidently that a higher number of filters in a bank implies a better recognition performance at the price of a higher computational complexity of the overall system. For comparison we also designed five filter banks of OTSDF filters and five filter banks of MOSSE filters, without using multi-objective optimization. All of these banks were designed to recognize the target and its distorted versions consisting of scaled versions by a factor within [0.8,1.2] and by in-plane rotation within the range of [-180,180] degrees. Note that the training images used for the design of MOSDF filters are chosen by the multi-objective optimization algorithm. Instead, the training images used for the design of OTSDF and MOSSE filters are chosen in an ad-hoc manner. We are interested to investigate the impact of the selection of training images to the performance of a composite filter. The training images for both OTSDF and MOSSE filters were chosen in such a way that each filter in the bank contains $180/n_B$ images, where n_B is the number of filters in the bank. So, a single filter in a bank of 30 filters will contain 6

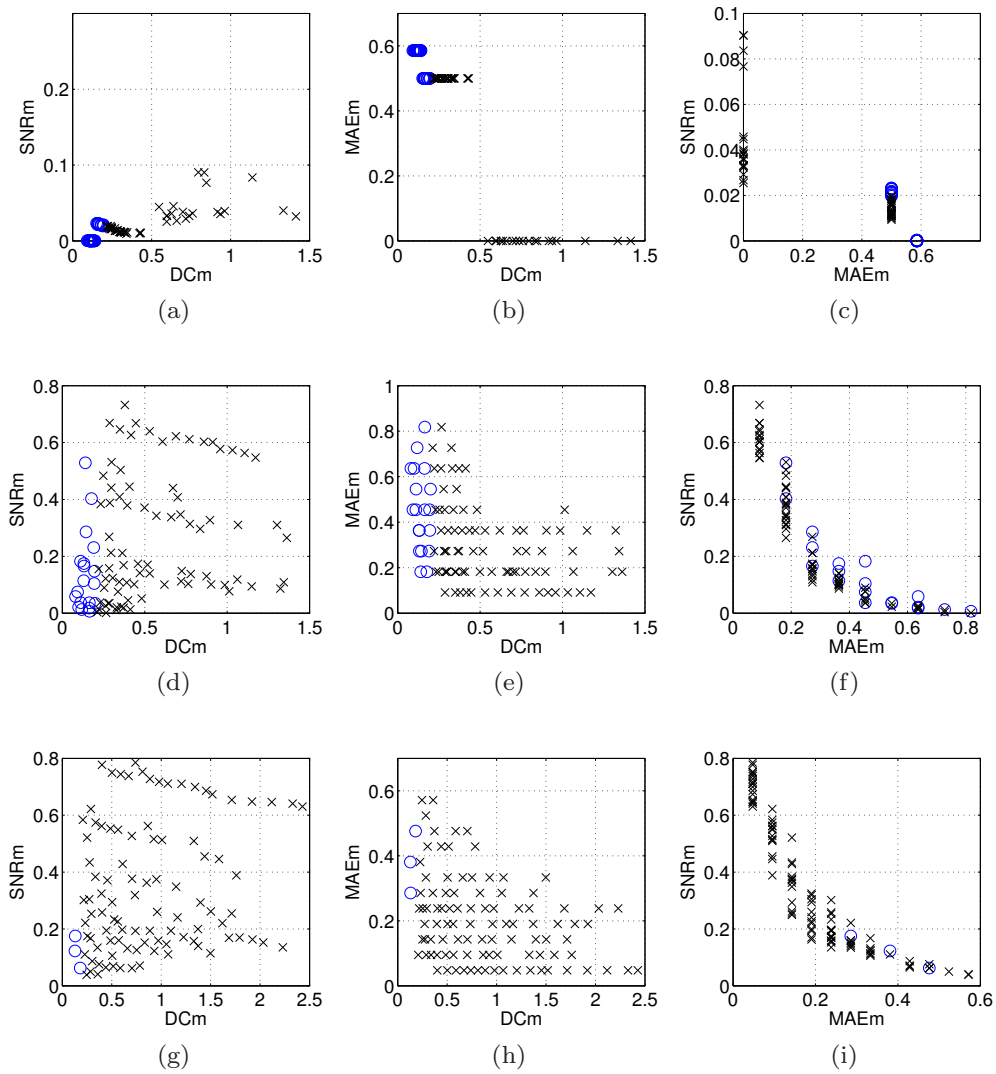

Figure 6: Pareto fronts obtained with the proposed multi-objective combinatorial algorithm for the design of filter banks of: (a)-(c) 30 filters, (d)-(f) 18 filters, (g)-(i) 5 filters.

training images, whereas a filter in a bank of 5 filters will contain 36 images. In order to find the best trade-off among target recognition performance and computational complexity, the algorithm in Fig. 4 can be used. The parameters for the multi-objective optimization algorithm are given as follows: 50 generations, populations of 200 individuals, archive size of 200 individuals, and 5% of mutation. Fig. 6 shows examples of the obtained Pareto sets for the design of MOSDF filters. The circles indicate MOSDF filter solutions that yield a DC value higher than 0.85. It can be seen, that the number of solutions satisfying $DC > 0.85$ is higher for the filter bank of 30 filters than for filter banks with less number of filters. Furthermore, it is evident from Fig. 6 that there is a trade-off between the DC and the MAE as well as between the DC and the SNR measures.

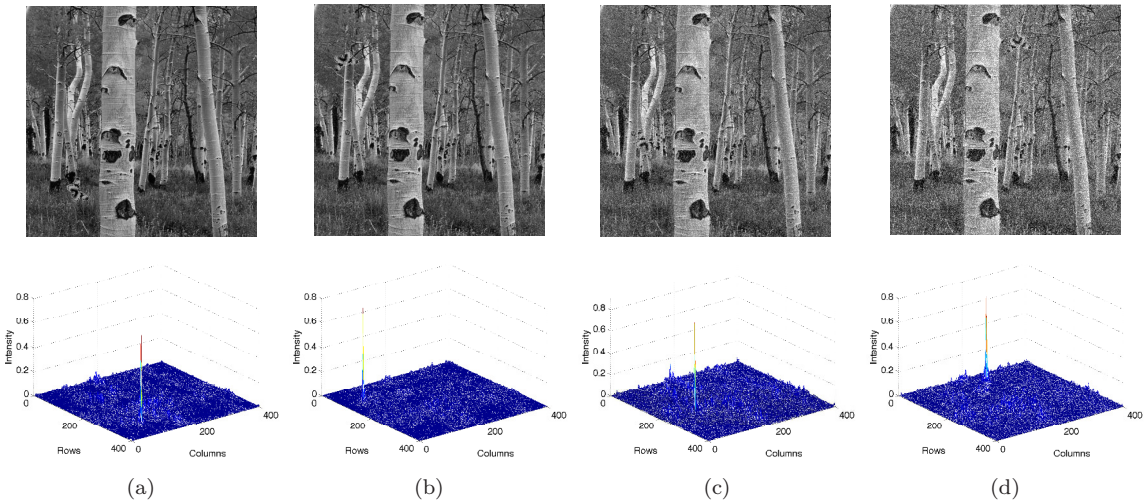

Figure 7: Examples of test scenes and correlation intensity planes obtained with a filter bank of 18 MOSDF filters, for target recognition in additive noise of: (a) 100 dB SNR; (b) 50 dB SNR; (c) 30 dB SNR; (d) 20 dB SNR.

Next, we evaluate the detection performance of all designed filter banks in 100 scenes for different positions and views of the target, and for various additive noise SNR values. Fig. 7 shows examples of test scenes for this experiment. The target can be randomly located within the scene with an arbitrary orientation and scaling inside the prescribed ranges. Fig. 7 also shows the correlation intensity plane for each scene obtained with the filter bank of 18 MOSDF filters. Note that a sharp correlation peak indicates the correct position of the target. With 95% confidence, the results in terms of the DC obtained with MOSDF, OTSDF, and MOSSE filters are presented in Fig. 8. It can be seen that the proposed MOSDF filters yield the best results in all the cases. Furthermore, we can observe that both OTSDF and MOSSE filter banks having 30, 18, and 12 filters exhibit a similar performance. However, the MOSSE filters yield a slightly better performance than that of the OTSDF filters for low noise of 100 dB and 50 dB SNR, whereas for 30 dB SNR and below the performance of the OTSDF filters is better than that of the MOSSE filters. Actually, the banks of 9 and 5 MOSSE filters are unable to detect the target (negative DC values) when the SNR of the additive noise is 10 dB. A similar situation occurs for the filter bank of 5 OTSDF filters. On the other hand, all MOSDF filters are able to recognize the target (DC>0) for all noise levels, even when only 5 filters are used and when the SNR of the noise is 10 dB.

Now, we evaluate the accuracy of location estimation of the target of all designed filter banks. With 95% confidence, the results obtained with MOSDF, OTSDF, and MOSSE filters in terms of LE, are presented in Fig. 9. It can be seen that the MOSDF, OTSDF, and MOSSE filter banks having 30 and 18 filters yield low LE values for noisy conditions of 100 dB, 50 dB, and 30 dB SNR. However, the OTSDF and MOSSE banks having 12, 9, and 5 filters yield high LE values, whereas the banks of MOSDF filters yield the lowest LE values. According with the obtained results, we can say that the OTSDF filters yield the best robustness to

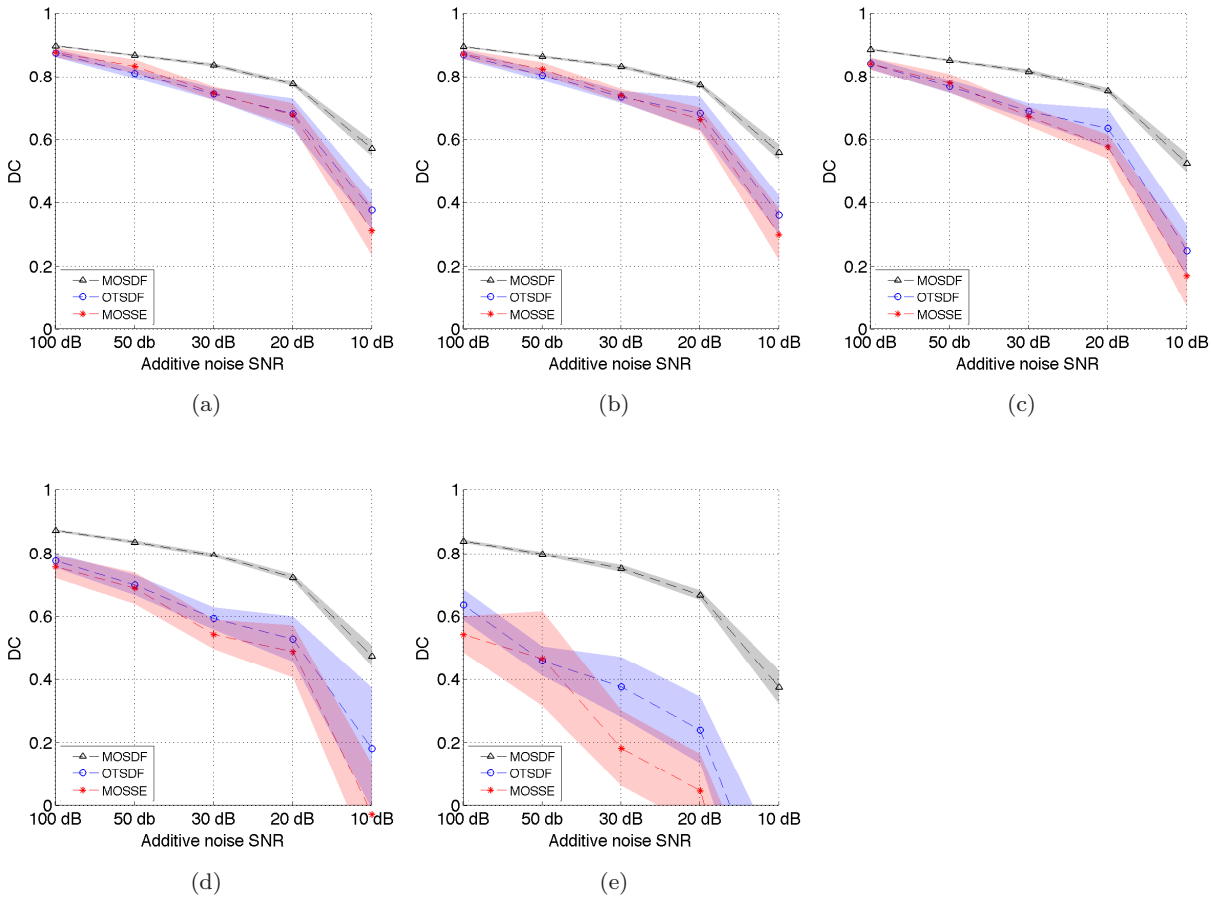

Figure 8: DC performance with 95% confidence obtained with MOSDF, OTSDF and MOSSE filter banks: (a) 30 filters, (b) 18 filters, (c) 12 filters, (d) 9 filters, (e) 5 filters.

additive noise, whereas the MOSSE filters yield the worst performance among all tested filters.

Next, we evaluate the performance of the designed filter banks in terms of efficiency of target recognition. In order to guarantee correctly statistical results, 100 tests were carried out for different positions and views of the target, and different additive noise SNR values. The target recognition systems based on MOSDF, OTSDF, and MOSDF filters work as follows. The input scene is firstly correlated with all filters of the bank and the correlation plane with the highest DC value is chosen. Next, if the DC of the chosen plane is greater than a threshold of 0.1 and the calculated LE of the chosen plane is less than half of the size of the target ($LE < 18$), then the target is detected; otherwise, the target is rejected. Fig. 10 shows the percentage of correctly target detections in 100 test scenes versus noise level for all considered filters. We can see that the proposed MOSDF filters yield the best results. Actually, the MOSDF filters are able to recognize the target with efficiency of 100% using 30, 18, 12, and 9 filters for all noise levels, and achieve a recognition rate of 94.2% when only 5 filters are used and the SNR of the additive noise is 10 dB. The filter bank of 30 OTSDF filters yields a recognition rate of 100% in environment of 100 dB, 50 dB, 30 dB, and 20 dB

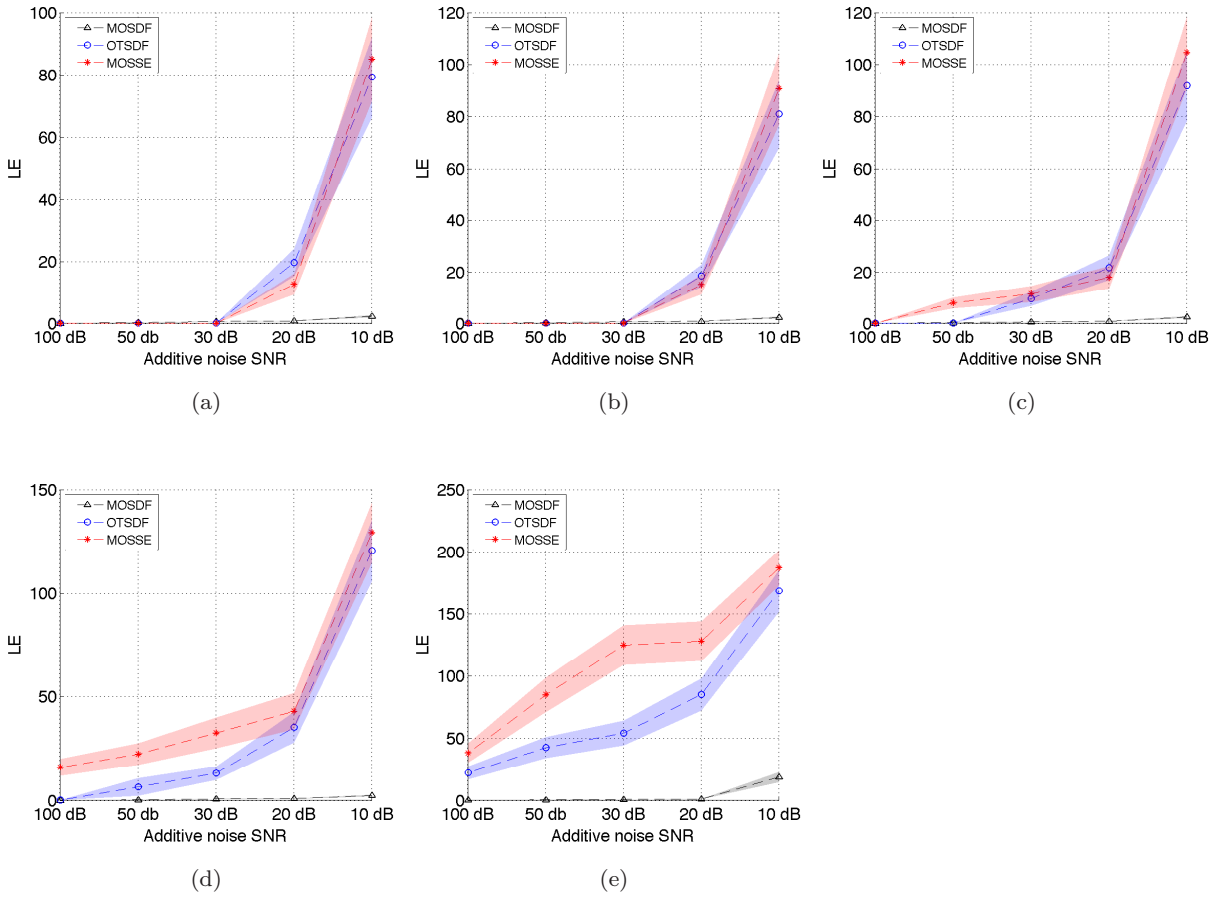

Figure 9: LE performance with 95% confidence obtained with MOSDF, OTSDF and MOSSE filter banks: (a) 30 filters, (b) 18 filters, (c) 12 filters, (d) 9 filters, (e) 5 filters.

SNR, and achieves a recognition rate of 92% in a highly noisy environment of 10 dB SNR. Nevertheless, the performance of the filter banks of 18, 12, 9, and 5 OTSDF filters is lower than that of MOSDF filter banks when the SNR of the additive noise decreases. The filter banks of 30, 18, 12, and 9 MOSSE filters yield a good recognition performance in noisy conditions of 100 dB, 50 dB, 30 dB, and 20 dB SNR. However, the performance of the MOSSE filters decreases considerably when the SNR of the additive noise is 10 dB. It can be seen that the proposed MOSDF filters yield the best detection rates with the minimum number of correlation filters.

We employed the binary-search procedure shown in Fig. 4 to construct filter banks of MOSDF, OTSDF, and MOSSE filters. We want to determine the minimum number of required filters to achieve a recognition performance satisfying $DC \geq 0.85$. For the case of MOSDF filters the minimum number of filters satisfying the DC condition is 9, whereas for both OTSDF and MOSSE filters the minimum number of required filters is 16. Note that these results are consistent with those shown in Fig. 8. This means that the suggested approach achieves the highest recognition performance with the lowest computational complexity.

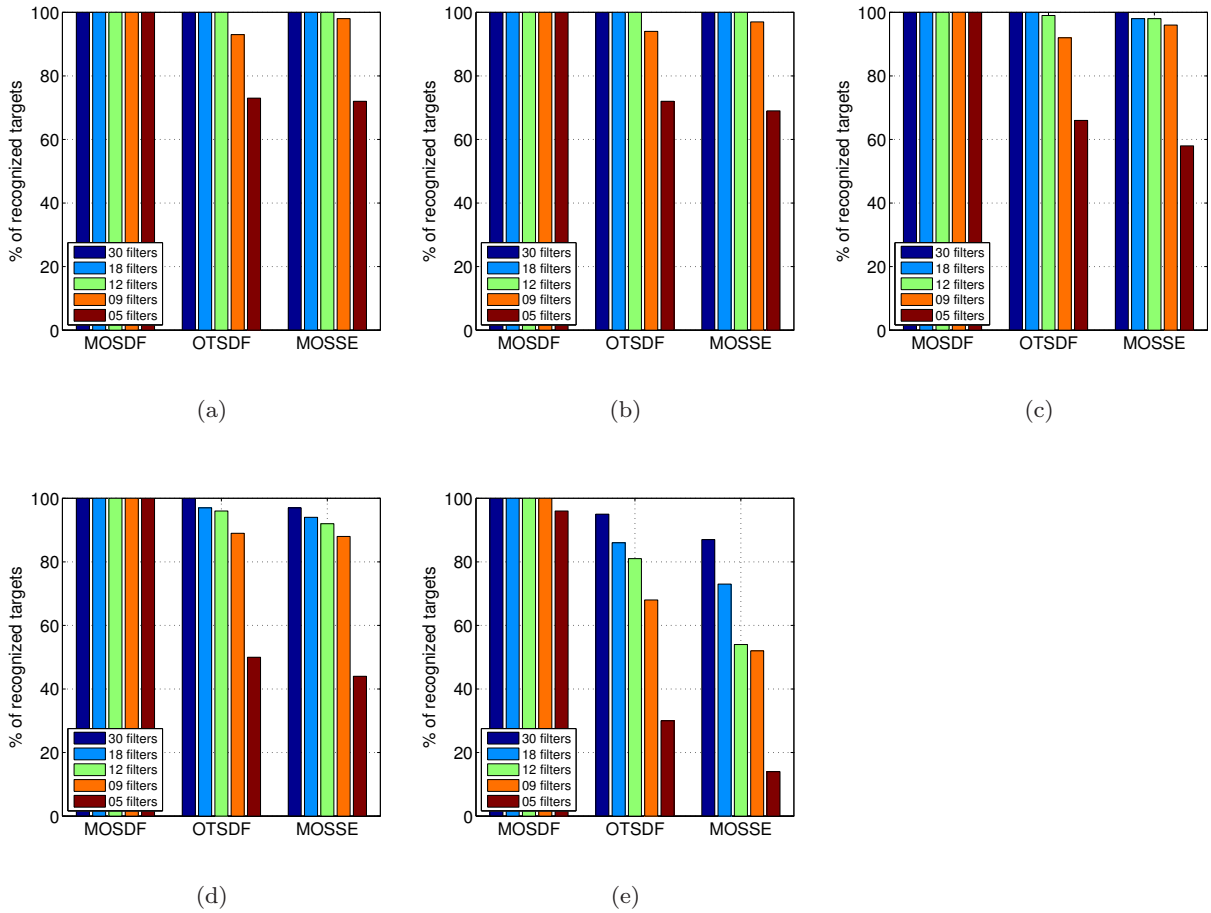

Figure 10: Detection efficiency of considered correlation filter in 100 scenes corrupted with additive noise with: (a) 100 dB SNR, (b) 50 dB SNR, (c) 30 dB SNR, (d) 20 dB SNR, (e) 10 dB SNR.

Now, we test the classification performance of the considered composite filters using face images from the Extended Yale Face Database B [39, 40]. This database consists of 39 sets of face images (one set for a different subject), where each set contains 64 monochrome images of 168×192 pixels. Fig. 11 shows examples of face images of different subjects of the database. We designed pattern recognition systems based on SDF, MOSDF, OTSDF, and MOSSE filters to detect and classify face images of ten different subjects. For this purpose, one filter bank for each of the considered filters were constructed. Each bank contains ten filters (one filter per subject). The MOSDF filters were designed using the suggested multi-objective algorithm shown in Fig. 2. Note that for the design of a single filter to recognize face images of one subject, 64 true-class images and 64×9 false-class images are available for the training process of the filter. In order to show the importance of a proper selection of the training images, the SDF, OTSDF and MOSSE filters were designed with all available true- and false-class images. This means that each SDF or OTSDF filter contains 64 true-class training images, and 576 false-class images, whereas each MOSSE filter contains 64 true-class training images. The number of training images chosen by the optimization algorithm in the design of MOSDF filters

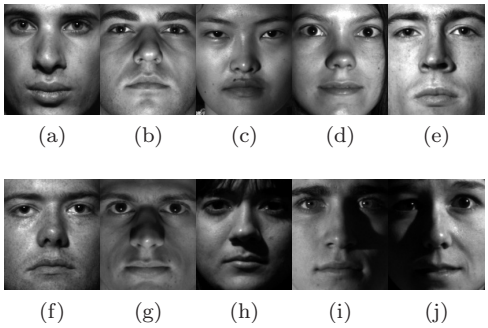

Figure 11: Examples of face images of the Extended Yale Face Database B used for pattern classification.

is 44 true-class images and 268 false-class training images (in average). This represents a reduction of 31.2% of true-class images and 53.4% of false-class images, comparing with the number of training images used for the design of SDF, OTSDF, and MOSSE filters. The face classification systems based on MOSDF, SDF, OTSDF and MOSSE filters operate as follows: the input image is firstly preprocessed using a histogram modification [41] to reduce the effects of inhomogeneous illumination. Afterwards, the corrected image is processed with each filter in the bank according with the diagram shown in Fig. 1. The correlation plane with the highest DC value among all filters in the bank is considered as the output plane of the bank. Next, a support vector machines (SVM) classifier [42], is used to decide if the input face is a target or an impostor. The SVM classifier utilizes as features the values of the DC and correlation peak of the output plane. The system assigns the detected face to the corresponding category of the filter that yields the highest DC value. Fig. 12 shows examples of the SVM classifier for one subject, obtained with each of the tested composite filters. We can see, that the proposed MOSDF filters yield the highest interclass separation (margin) and exhibit the better intraclass compaction. Next, we compute the confusion matrix for each filter bank for 640 face images corrupted with additive noise of 100 dB, 50 dB, 20 dB, 10 dB, and 5 dB SNR. These matrices show the percentage of decisions (classifications) made by the system versus the number of input faces per subject. Examples of the obtained confusion matrices for MOSDF, SDF, and OTSDF filters are presented in Fig. 13. It can be seen, that for additive noise SNR of 100 dB the MOSDF and OTSDF filters with correctly classification rates of 98.4% and 100%, respectively, yield the best results. It is interesting to note by comparing the performance of the basic SDF filter (Fig. 13(b)) with the performance of the MOSDF filter (Fig. 13(a)), that the MOSDF filters yield significantly lower classification errors, by performing a better selection of the training images during the filter design. This effect is more evident when comparing the classification results for low SNR values of additive noise (compare Fig. 13(e) with Fig. 13(f), and Fig. 13(i) with Fig. 13(j)). One can observe that the OTSDF filters yield a slightly better performance than that obtained with the MOSDF filters when the effect of additive noise is negligible (100 dB SNR). However, when the SNR of noise decreases the performance of the OTSDF filters is significantly lower than that of the MOSDF filters. This can be seen by comparing Fig. 13(e) with Fig. 13(g), and Fig. 13(i) with Fig.

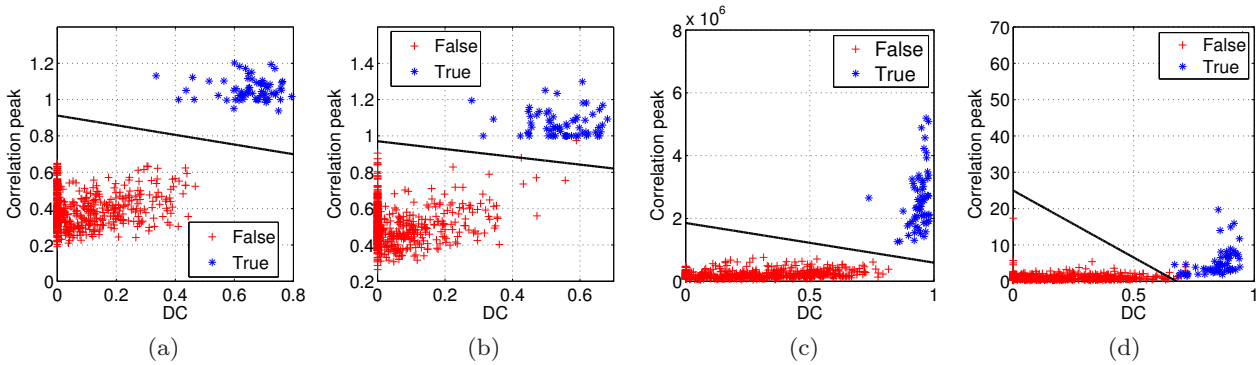

Figure 12: Examples of SVM classifier for 640 face images. (a) MOSDF, (b) SDF, (c) OTSDF, (d) MOSSE.

13(k). An interesting behavior of OTSDF filters is that for additive noise levels of 100 dB, 50 dB, and 20 dB SNR, the filters only yield rejection errors (see Fig. 13(c) and (g)). The MOSSE filters exhibit the worst classification performance among all tested filters. Actually, the MOSSE filters only perform well when the effect of additive noise is negligible.

Finally, Fig. 14 summarizes the classification performance of the tested filters given in terms of rates of positive classifications, false positive errors, and rejections. We can see from Fig. 14(a) that all tested filters perform well when the additive noise is negligible. However, from 20 dB SNR and below the rate of correct classifications of OTSDF and MOSSE filters decreases considerably, while the proposed MOSDF filters maintains high performance rates. The OTSDF filters yield low rates of misclassification errors for additive noise levels of 100 dB, 50 dB, and 20 dB SNR at the price of high rate of rejection errors. Finally, we can conclude that the proposed approach for the design of composite correlation filters is effective for pattern recognition.

4.1. Conclusions

A new optimization algorithm for the design of composite correlation filters for distortion invariant target recognition was presented. The algorithm combines a multi-objective evolutionary strategy (SPEA2) in conjunction with a variable length crossover and coding technique (SAGA) to synthesize a filter bank of SDF filters with an optimized performance in terms of DC, MAE and SNR metrics. A filter bank of optimized filters can be designed by means of the suggested binary-search-based algorithm. This algorithm allows the construction of a filter bank by maximizing the pattern recognition performance while minimizing the computational complexity of the overall system. Given a vast search space of feasible true- and false-class templates, the proposed algorithm finds a subset of these templates that allows the synthesis of composite filters with an optimized performance in terms of a trade-off among several conflicting criteria. The obtained results showed that the proposed multi-objective composite filters yield a better recognition performance in terms of the DC and LE measures than that obtained with OTSDF and MOSSE filters. The composite

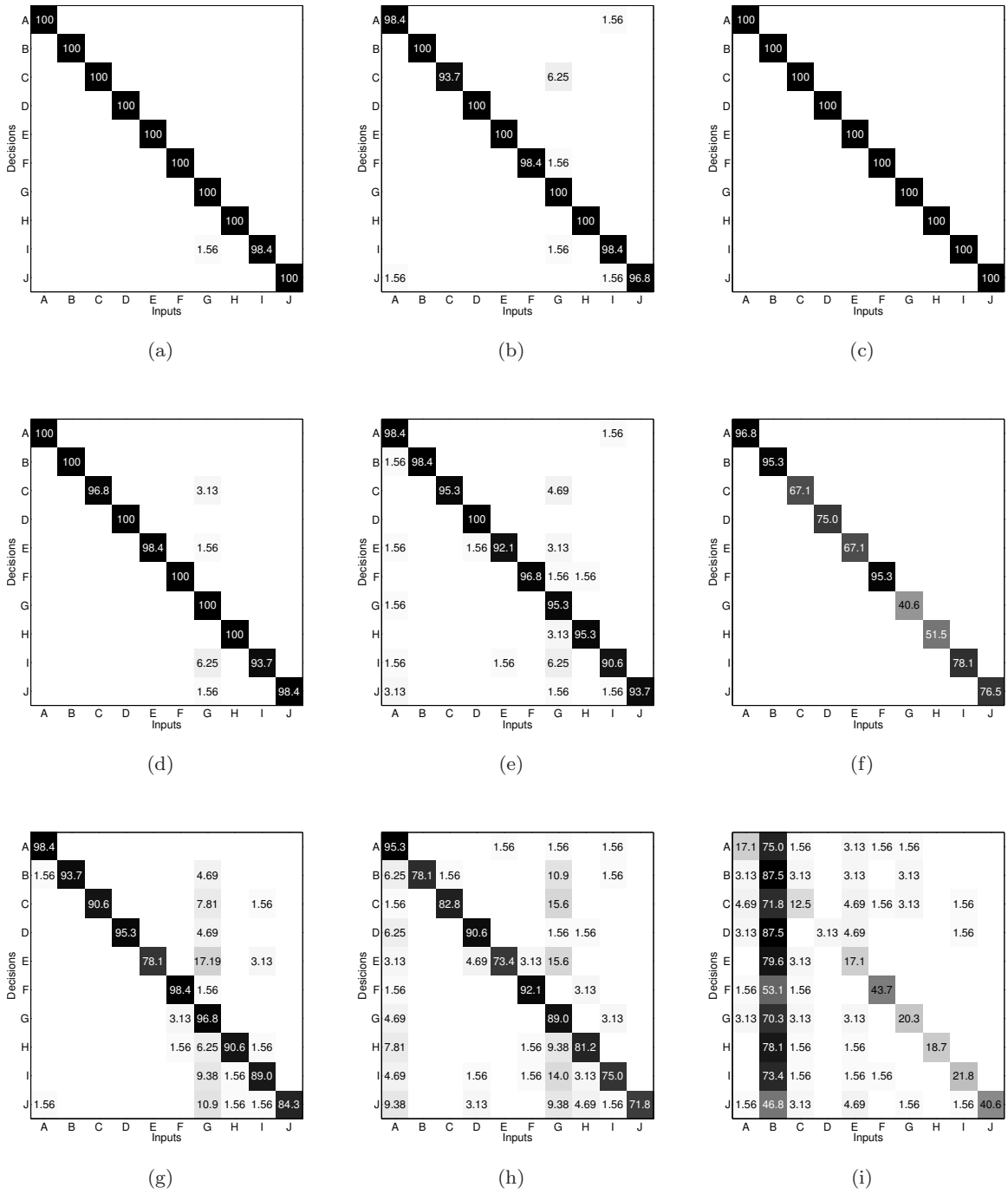

Figure 13: Confusion matrices of MOSDF, SDF, and OTSDF filters in face classification. First row ((a)-(d)): MOSDF, SDF, and OTSDF filters in environment of additive noise with 100 dB SNR. Second row ((e)-(h)): MOSDF, SDF, and OTSDF filters in environment of additive noise with 20 dB SNR. Third row ((i)-(l)): MOSDF, SDF, and OTSDF filters in environment of additive noise with 5 dB SNR.

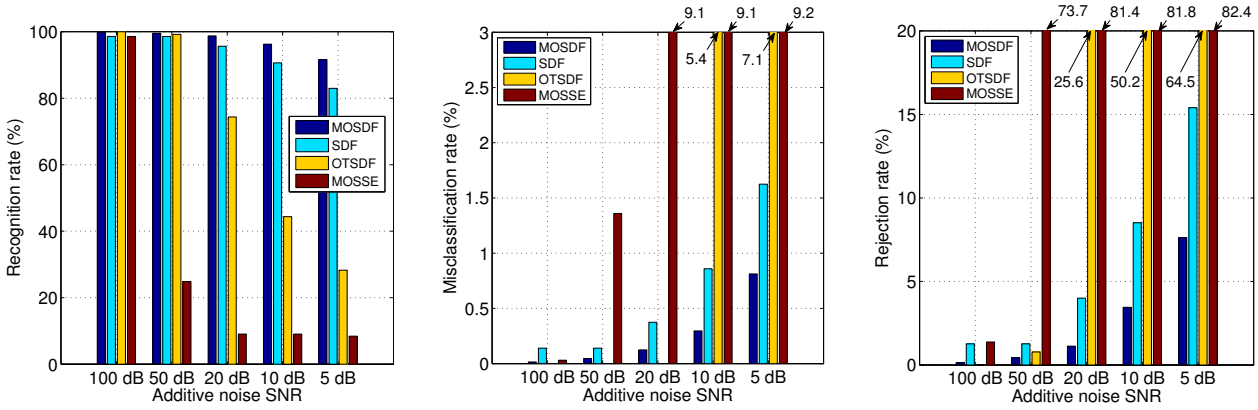

(a) (b) (c)

Figure 14: Performance of MOSDF, SDF, OTSDF, and MOSSE filters in face classification. (a) percentages of correctly classifications, (b) percentages of misclassification errors (no decision), (c) percentages of rejection errors.

filters synthesized with the proposed approach have exhibited a robust behavior in highly noisy conditions for target recognition and classification problems.

References

[1] R. O. Duda, P. E. Hart, D. G. Stork, Pattern Classification, John Wiley and Sons, 2001.
[2] S. Theodoridis, K. Koutroumbas, Pattern Recognition, Fourth Edition, 4th Edition, Academic Press, 2008.
[3] D. G. Lowe, Distinctive image features from scale-invariant keypoints, Int. J. Comput. Vision 60 (2) (2004) 91–110.
[4] T. Tuytelaars, K. Mikolajczyk, Local invariant feature detectors: A survey, Found Trends Comp. Graphics and Vision (2008) 177–280.
[5] H. Bay, A. Ess, T. Tuytelaars, L. V. Gool, Speeded up robust features, Comp. Vis. image underst. 110 (2008) 346–359.
[6] J. Li, Y. Wang, Y. Wang, Visual tracking and learning using speeded up robust features, Pattern Recogn. Lett. 33 (16) (2012) 2094–2101.
[7] V. H. Diaz-Ramirez, O. G. Campos-Trujillo, V. Kober, P. M. Aguilar-Gonzalez, Multiclass pattern recognition using adaptive correlation filters with complex constraints, Opt. Eng. 51 (3) (2012) 037203–1–037203–12.
[8] P. M. Aguilar-Gonzalez, V. Kober, Design of correlation filters for pattern recognition using a noisy reference, Opt. Comm. 285 (5) (2012) 574 – 583.
[9] M. Brown, G. Hua, S. Winder, Discriminative learning of local image descriptors, IEEE Trans. Pattern Anal. Mach. Intell. 33 (1) (2011) 43–57.
[10] G. Olague, L. Trujillo, Evolutionary-computer-assisted design of image operators that detect interest points using genetic programming, Image Vision Comput. 29 (7) (2011) 484–498.
[11] V. H. Diaz-Ramirez, V. Kober, Target recognition under nonuniform illumination conditions, Appl. Opt. 48 (2009) 1408–1418.
[12] T. Manzurv, J. Zeller, S. Serati, Optical correlator based target detection, recognition, classification, and tracking, Appl. Opt. 51 (2012) 4976–4983.
[13] Y. Ouerhani, M. Jridi, A. Alfalou, C. Brosseau, Optimized pre-processing input plane GPU implementation of an optical face recognition technique using a segmented phase only composite filter, Opt. Comm. 289 (2013) 33 – 44.
[14] A. A. S. Awwal, K. L. Rice, T. M. Taha, Hardware accelerated optical alignment of lasers using beam-specific matched-filters, Appl. Opt. 48 (2009) 5190–5196.
[15] F. Chan, T. Towghi, B. Javidi, Distortion tolerant minimum mean squared error filter for detecting noisy targets in enviromental degradations, Opt. Eng. 39 (2000) 2092–2100.
[16] E. M. Ramos-Michel, V. Kober, Design of correlation filters for recognition of linearly distorted objects in linearly degraded scenes, J. Opt. Soc. Am. A. 24 (2007) 3403–3417.
[17] V. Kober, J. Campos, Accuracy of location measurement of a noisy target in a nonoverlapping background, J. Opt. Soc. Am. A 13 (8) (1996) 1653–1666.
[18] B. V. K. Vijaya-Kumar, L. Hassebrook, Performance measures for correlation filters, Appl. Opt. 29 (1990) 2997–3006.
[19] M. S. Alam, A. Bal, E. Horache, S.-F. Goh, C. H. Loo, S. P. Regula, A. Sharma, Metrics for evaluating the performance of joint-transform-correlation-based target recognition and tracking algorithms, Opt. Eng. 44 (6) (2005) 067005.
[20] B. V. K. Vijaya-Kumar, A. Mahalanobis, R. D. Juday, Correlation Pattern Recognition, Cambridge University Press, 2005.

[21] R. A. Kerekes, B. V. K. Vijaya-Kumar, Selecting a composite correlation filter design: a survey and comparative study, Opt. Eng. 47 (6) (2008) 067202.
[22] B. V. K. Vijaya-Kumar, Tutorial survey of composite filter designs for optical correlators, Appl. Opt. 31 (1992) 4773–4801.
[23] A. Mahalanobis, B. V. K. Vijaya-Kumar, S. Song, S. R. F. Sims, J. F. Epperson, Unconstrained correlation filters, Appl. Opt. 33 (17) (1994) 3751–3759.
[24] B. V. K. Vijaya-Kumar, E. Pochapsky, Signal-to-noise ratio considerations in modified matched spatial filters, J. Opt. Soc. Am. A 3 (6) (1986) 777–786.
[25] E. Zitzler, M. Laumanns, L. Thiele, Spea2: Improving the strength pareto evolutionary algorithm for multiobjective optimization, in: Evolutionary Methods for Design, Optimisation, and Control, CIMNE, Barcelona, Spain, 2002, pp. 95–100.
[26] I. Harvey, The saga cross: The mechanics of recombination for species with variable-length genotypes, in: In R. Manner & B. Manderick, (Eds.), Parallel Problem, North-Holland, 1992, pp. 269–278.
[27] C. F. Hester, D. Casasent, Multivariant technique for multiclass pattern recognition, Appl. Opt. 19 (1980) 1758–1761.
[28] F. Goudail, P. Refregier, Statistical Image Processing Techniques for Noisy Images, an application-oriented approach, Kluwer Academic, Boston, 2004.
[29] D. S. Bolme, J. R. Beveridge, B. A. Draper, Y. M. Lui, Visual object tracking using adaptive correlation filters, in: CVPR, 2010, pp. 2544–2550.
[30] R. A. Kerekes, B. V. K. Vijaya-Kumar, Correlation filters with controlled scale response, IEEE Trans. Imag. Proc. 15 (7) (2006) 1794–1802.
[31] B. V. K. Vijaya-Kumar, A. Mahalanobis, A. Takessian, Optimal tradeoff circular harmonic function correlation filter methods providing in-plane rotation response, Appl. Opt. 9 (6) (2000) 1025–1034.
[32] B. V. K. Vijaya-Kumar, D. W. Carlson, A. Mahalanobis, Optimal trade-off synthetic discriminant function filters for arbitrary devices, Opt. Lett. 19 (19) (1994) 1556–1558.
[33] C. A. C. Coello, G. B. Lamont, D. A. V. Veldhuizen, Evolutionary Algorithms for Solving Multi-Objective Problems (Genetic and Evolutionary Computation), Springer-Verlag New York, Inc., 2006.
[34] J. H. Holland, Adaptation in Natural and Artificial Systems: An Introductory Analysis with Applications to Biology, Control and Artificial Intelligence, MIT Press, 1992.
[35] A. Zhou, B. Qu, H. Li, Z. Zhao, P. Suganthan, Q. Zhang, Multiobjective evolutionary algorithms: A survey of the state of the art, Swarm and Evolutionary Computation 1 (1) (2011) 32 – 49.
[36] E. Zitzler, M. Laumanns, L. Thiele, SPEA2: Improving the strength pareto evolutionary algorithm for multiobjective optimization, in: Evolutionary Methods for Design Optimization and Control with Applications to Industrial Problems, International Center for Numerical Methods in Engineering, Athens, Greece, 2001, pp. 95–100.
[37] E. Zitzler, L. Thiele, Multiobjective evolutionary algorithms: A comparative case study and the strength pareto approach.
[38] Z. Michalewicz, D. B. Fogel, How to solve it : modern heuristics, Springer, New York, 2000.
[39] A. Georghiades, P. Belhumeur, D. Kriegman, From few to many: Illumination cone models for face recognition under variable lighting and pose, IEEE Trans. Pattern Anal. Mach. Intelligence 23 (6) (2001) 643–660.
[40] K. Lee, J. Ho, D. Kriegman, Acquiring linear subspaces for face recognition under variable lighting, IEEE Trans. Pattern Anal. Mach. Intelligence 27 (5) (2005) 684–698.
[41] V. Struc, J. Zibert, N. Pavesic, Histogram remapping as a preprocessing step for robust face recognition, WSEAS transactions on information science and applications 6 (3) (2009) 520–529.
[42] C. Cortes, V. Vapnik, Support-vector networks, Mach. Learn. 20 (3) (1995) 273–297.

Prepared by LLNL under Contract DE-AC52-07NA27344.